Integrative and Comparative Biology

Integrative and Comparative Biology, volume 58, number 2, pp. 251–260
doi:10.1093/icb/icy049

Society for Integrative and Comparative Biology

SYMPOSIUM

Myofascial Loads Can Occur without Fascicle Length Changes

Chris Tijs,[*] Michel Bernabei,[†] Jaap H. van Dieën[‡] and Huub Maas[1,‡]

[*]Department of Organismic and Evolutionary Biology, Concord Field Station—Harvard University, Bedford, MA 01730, USA; [†]Department of Biomedical Engineering, Northwestern University, Evanston, IL 60208, USA; [‡]Department of Human Movement Sciences, Faculty of Behavioural and Movement Sciences, Vrije Universiteit Amsterdam, 1081 BT, Amsterdam, The Netherlands

From the symposium "Spatial Scale and Structural Heterogeneity in Skeletal Muscle Performance" presented at the annual meeting of the Society for Integrative and Comparative Biology, January 3–7, 2018 at San Francisco, California.

[1]E-mail: h.maas@vu.nl

Synopsis Many studies have shown that connective tissue linkages can transmit force between synergistic muscles and that such force transmission depends on the position of these muscles relative to each other and on properties of their intermuscular connective tissues. Moving neighboring muscles has been reported to cause longitudinal deformations within passive muscles held at a constant muscle–tendon unit (MTU) length (e.g., soleus [SO]), but muscle forces were not directly measured. Deformations do not provide a direct measure of the force transmitted between muscles. We combined two different muscle preparations to assess whether myofascial loads exerted by neighboring muscles result in length changes of SO fascicles. We investigated the effects of proximal MTU length changes of two-joint gastrocnemius (GA) and plantaris (PL) muscles on the fascicle length of the one-joint SO muscle within (1) an intact muscle compartment and (2) a disrupted compartment that allowed measurements of fascicle length and distal tendon force of SO simultaneously. SO muscle bellies of Wistar rats ($n = 5$) were implanted with sonomicrometry crystals. In three animals, connectivity between SO and GA+PL was enhanced. Measurements were performed before and during maximal excitation of all plantar flexor muscles. In both setups, MTU length of GA+PL did not affect the length of SO fascicles, neither during passive nor active conditions. However, lengthening the MTU of GA+PL increased distal tendon force of SO by 43.3–97.8% ($P < 0.001$) and 27.5–182.6% ($P < 0.001$), respectively. This indicates that substantial myofascial force transmission between SO and synergistic muscle can occur via a connective tissue network running parallel to the series of SO sarcomeres without substantial length changes of SO fascicles.

Introduction

To control body movements, forces exerted by skeletal muscles must be transmitted to the skeleton. For isolated muscles, forces can be exerted only via tendinous structures at the muscle origin and insertion. However, within an intact muscle compartment, forces can be exerted directly onto the muscle belly surface (the epimysium) of neighboring muscles mediated by connective tissues linking them (Huijing 2009; Maas and Sandercock 2010). Such so called epimuscular myofascial loads have been shown in rats to cause unequal forces measured at the muscles' origin and insertion (Huijing and Baan 2001; Maas et al. 2001) and were found to be dependent on the length (Maas et al. 2001; Maas and Huijing 2009) and position (Maas et al. 2004) of a single muscle relative to adjacent muscles. More recently, scar tissue formation after a tendon transfer surgery (Maas and Huijing 2011, 2012a, 2012b) and enhanced stiffness of the intermuscular connective tissues (Bernabei et al. 2016, 2017a) has been shown to affect the magnitude of epimuscular myofascial loads. These results indicate the potential importance of force transmission via myofascial pathways for pathological conditions.

It is well-known that skeletal muscles can deform along its long axis as well as radially in response to muscle activation and joint movements. Recent studies in humans (Bojsen-Møller et al. 2010; Tian et al. 2012; Finni et al. 2017) and rats (Tijs et al. 2015a) have shown that longitudinal muscle deformations can also be caused by myofascial loads. Passive

Advance Access publication June 4, 2018

knee flexion was found to increase the length of passive soleus (SO) fascicles in humans (Tian et al. 2012) and change the length of in-series sarcomeres locally within passive fibers of the tibialis anterior muscle in rats (Tijs et al. 2015a). The muscles in these studies do not span the knee joint. Therefore, results cannot be ascribed to changes in their muscle–tendon unit (MTU) length, but are more likely the result of myofascial loads.

The mechanical consequences of these longitudinal length changes are unknown as no study has yet measured muscle forces and deformations due to myofascial loads simultaneously. Theoretically, an altered distribution of fiber mean sarcomere length would change the shape of the muscle length–force relationship, i.e., the range of active force exertion and optimal force (Huijing 1995). Thus, longitudinal length changes due to myofascial loads may cause changes in the force generating capacity of muscles. Despite the absence of experimental evidence, finite element models of linked muscles have predicted myofascial loads to cause local variation in strains as well as stresses within the muscle belly (Yucesoy and Huijing 2012). Thus, the question is whether myofascial loads originate purely from force transmission from neighboring muscles or that they affect the force generating capacity of a muscle.

The aim of the present study was to experimentally assess whether myofascial loads exerted by neighboring muscles result in length changes of SO fascicles. Specifically, we investigated the effects of relative muscle displacement of two-joint gastrocnemius (GA) and plantaris (PL) muscles on fascicle length changes of one-joint SO muscle within an intact muscle compartment of the rat and within a disrupted compartment that allowed additional measurements of accompanying forces exerted at the distal tendon of SO. Because the magnitude of myofascial loads is affected by the stiffness of intermuscular connective tissues (Bernabei et al. 2017a), we ensured a wide range in intermuscular connectivity by enhancing connectivity through implantation of a tissue-integrating mesh for a subset of the animals. Because muscle fascicle stiffness is dependent on the level of muscle activation, myofascial effects were assessed for fully passive and maximally activated plantar flexion muscles.

Materials and methods

Animal care

The experiments described here were part of a larger study assessing effects of changes in intermuscular connectivity on the mechanical interaction between plantar–flexor muscles (Bernabei et al. 2017a, 2017b). The original study consisted of survival surgeries for sensor implantation and for manipulation of intermuscular connectivity as well as the terminal experiment reported here. Five male Wistar rats (*Rattus norvegicus*; Berkenhout 1769), body mass at the time of terminal experiment (378 ± 12 g) were tested in this study. Survival surgeries were performed in aseptic conditions, using inhalation anesthesia (2–3% isoflurane) and a one-time pre-operative subcutaneous injection of a painkiller (0.02 mg/kg; Temgesic; Schering-Plough, Maarssen, The Netherlands). Additional doses were given 1–2 days after the surgery if signs of pain were noticed. For the terminal experiments, animals were anesthetized by an intraperitoneal injection of urethane solution (1.2 mL/100 g body mass, 12.5% urethane solution). On completion of measurements, animals were euthanized with a pentobarbital overdose (Euthasol 20%) injected intracardially, followed by a double-sided pneumothorax. All surgical and experimental procedures were approved by the Committee on the Ethics of Animal Experimentation at the Vrije Universiteit Amsterdam and in strict agreement with the guidelines and regulations concerning animal welfare and experimentation set forth by Dutch law.

Muscle anatomy

The anatomy of the plantar flexor muscles in rats has been well characterized (Greene 1935). In brief, GA muscle consists of a medial and lateral (LG) head that originate from the medial and lateral epicondyle of the femur, respectively. In contrast, SO arises from the head of the fibula. Both muscles insert on the calcaneus bone via the shared Achilles tendon. Although the Achilles tendon is typically considered as one entity, relative displacement and differential strains can occur between its subtendons (Finni et al. 2018). PL also originates from the lateral epicondyle, but its distal tendon wraps around the calcaneus and inserts on the phalanx of the digits via the flexor digitorum brevis muscle. Changes in knee joint angle will result in changes in MTU length of GA+PL as well as changes in the position of these muscles relative to SO. Although SO and GA can be seen as distinct muscles, connective tissue linkages between SO and LG are present along the entire SO muscle belly length. These linkages can be divided into a proximal and a distal part with respect to a neurovascular tract, which runs centrally between SO and LG muscle bellies (for schematic drawings see Bernabei et al. 2016).

Survival surgeries

The right hindlimb of all animals was surgically instrumented with sonomicrometry crystals (1 mm; Sonometrics, London, Ontario, Canada) using procedures previously reported in (Maas et al. 2009; Bernabei et al. 2017c). In short, a partial resection of the insertion sheath of the biceps femoris muscle was performed to access the compartment of SO and LG+PL muscles. A partial crural fasciotomy from the lateral side exposed the proximal two-thirds of SO and LG muscles. Distally, the biceps femoris sheath was lifted, exposing the distal portions of SO and LG muscle bellies converging in the Achilles tendon. Pockets for sonomicrometry crystals were made as close as possible to the proximal and distal myotendinous junctions (MTJs), limiting damage to intermuscular connective tissues. Crystal positioning sites allowed us to measure the muscle belly lengths of LG (L_{LG}) and SO (L_{SO}). Because of the small pennation angle and parallel fibered architecture of SO (Close 1964; Eng et al. 2008), these measurements were assumed to be representative of SO fascicle lengths. After the skin had been sutured, the animals were allowed to recover for 2 weeks prior to connectivity manipulation surgery.

In three animals (TI-1, TI-2, and TI-3), the intermuscular connectivity between the muscle bellies of SO and the lateral GA and PL complex (LG+PL) was enhanced by implanting a surgical mesh for tissue-integration with procedures previously reported in detail (Bernabei et al. 2017a). Connective tissues between the dorsal side of SO and the ventral side of LG+PL were bluntly dissected and a tissue-integrating mesh (Premilene mesh; B. Braun Melsungen) was sutured to the SO muscle over two-thirds of its muscle belly, at the interface between SO, LG, and PL muscles. In two control animals (CO-4, CO-5) intermuscular connective tissues were left intact for comparison with physiological conditions. Terminal experiments were performed 4 weeks after the surgical procedures for mesh implantation.

Terminal experiments

Each animal was tested in two experimental setups: one in which all muscles were left attached to the skeleton and length changes were obtained by changes in ankle and knee joint angle (Tijs et al. 2014, 2015b), and one in which the tendons were connected to force transducers and length changes were obtained by repositioning the force transducers mimicking changes in ankle and knee joint angle (for details see Bernabei et al. 2015).

Joint angle set-up

Surgery

The skin and biceps femoris muscle of the right hindlimb were removed and the femur was exposed for attachment of a metal clamp. Tissues between the malleoli and Achilles tendon were removed to secure the calcaneus to the set-up. The sciatic nerve was partly dissected free for placement of a cuff electrode and crushed proximal to the cuff electrode to prevent muscle excitation via spinal reflexes. All branches of the sciatic nerve were left intact, therefore simultaneous stimulation of GA, PL, and SO muscles was performed.

Fixation to the experimental set-up

The right hindlimb was secured to the experimental set-up by clamping the femur and the foot. Ankle and knee joints were aligned with the set-up's rotational axes. The set-up allowed for manipulation of knee and ankle joint angles in the sagittal plane, while the angles around the two other axes were kept at 0° (Fig. 1A).

Experimental protocol

GA, PL, and SO muscles were excited maximally by supramaximal stimulation of the sciatic nerve (amplitude: 0.4–1.0 mA, frequency: 100 Hz, pulse width: 100 μs, duration: 500 ms) via the bipolar cuff electrode connected to a constant current source (Digitimer DS3, Digitimer Ltd., Hertfordshire, UK). Two experimental protocols were applied. First, the ankle angle was set to 90° while a wide range of knee angles was imposed (between 70° and 130°). As a result, SO was kept at a constant MTU length (because it spans only the ankle joint) while the MTU length of GA and PL muscles was estimated to change by ~3–4 mm (Johnson et al. 2008). Because the MTU length of SO was kept constant, any change in L_{SO} was considered as indications of myofascial loads. Secondly, the knee angle was set to 90° and the ankle angle was varied between 70° and 130°, which was estimated to result in MTU length changes of ~4 mm of all plantar–flexor muscles (Johnson et al. 2008). During the isometric contraction at each combination of ankle and knee joint angles, L_{SO} and L_{LG} were recorded using the implanted sonomicrometry crystals.

Tendon force set-up

Surgery

Following the joint angle manipulation protocols, medial gastrocnemius (MG) was removed by

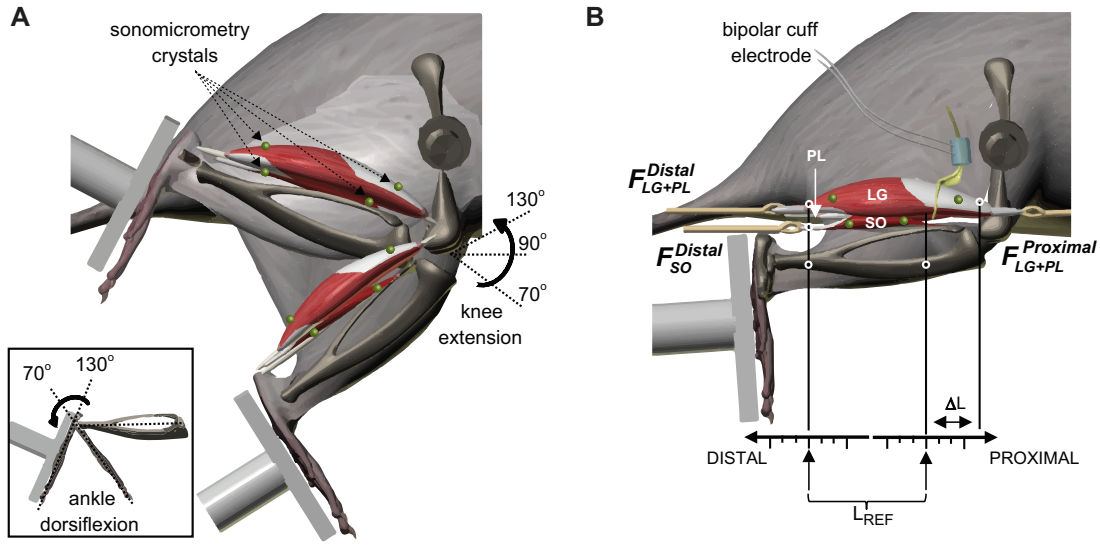

Fig. 1 Overview of the two experimental setups. The femur was fixed with a metal clamp and the foot was attached to a metal plate with custom-made clamps. A bipolar cuff electrode was placed on the sciatic nerve. The sites of sonomicrometry crystal implants in soleus (SO) and lateral gastrocnemius (LG) are shown (green dots). (**A**) Lateral view of the right hindlimb of the rat in the joint angle set-up, which allowed ankle and knee joints to be manipulated seperately. (**B**) Lateral view of the right hindlimb of the rat in the tendon-force setup. Proximal and distal tendons of lateral gastrocnemius and PL (LG+PL) as well as the distal tendon of SO were connected to separate force transducers. Proximal displacement of LG+PL and distal displacement of LG+PL+SO (ΔL) were expressed relative to the muscle–tendon unit lengths corresponding to 90°–90° knee–ankle joint angles (L_{REF}), identified with five reference markers (white circles) applied on the tendons and on the anterior tibial compartment. Forces were measured simultaneously at the proximal and distal tendons of LG+PL as well as at the distal tendon of SO.

carefully cutting the fibers that insert onto the medial side of the distal aponeurosis, which is shared with LG, in order to prevent damage to LG muscle fibers. This was done to prevent unphysiological strain between MG and LG as the MTU length of only LG+PL was changed proximally (see the "Experimental protocol" section). The SO, LG, and PL muscle group was dissected free from surrounding structures to exclude force transmission outside the muscle compartment, while preserving myofascial connections at the interface between the muscle bellies of SO and LG+PL. The distal tendon of SO was carefully dissected free from the rest of the Achilles tendon. Kevlar wires were used to connect the proximal and distal tendons of LG+PL as well as the distal tendon of SO to force transducers, which were positioned in such a way that forces could be measured in the muscle's line of pull, and that the relative position of muscles and tendons mimicked those present during normal joint movements.

Fixation to the experimental set-up

The rat was mounted in the experimental setup (Fig. 1B) by clamping the femur and the foot such that knee and ankle joints were kept at 90°, which was defined as the reference position (L_{REF}). Markers were placed near the distal MTJ of SO and near the proximal and distal MTJ of LG+PL. This enabled us to identify the position of the distal tendons of SO and LG+PL corresponding to L_{REF} for an ankle angle at 90°, and the position of the proximal tendons of LG+PL corresponding to L_{REF} for a knee angle at 90°. Applied MTU length changes were expressed relative to L_{REF} (ΔL in Fig. 1B). On completion of measurements, pictures of the implant were taken on the euthanized animal to verify consistent positioning of sonomicrometry crystals and for measuring inter-crystal distances as well as proximal and distal crystal-to-MTJ distances.

Experimental protocol

Isometric forces exerted at all three tendons were measured simultaneously for different lengths and relative positions of LG+PL and SO muscles. Two different protocols were applied: one to simulate MTU length changes during knee extension and one to simulate MTU length changes during ankle dorsiflexion. In the former, the proximal tendons of LG+PL were repositioned in steps of 1 mm from L_{REF} −3 mm, corresponding to ∼45° knee angle, to L_{REF} +3 mm, corresponding to ∼130° knee angle, while the distal tendons of SO and LG+PL were kept at L_{REF}, so that MTU length of SO was constant. Therefore, any change in L_{SO} was considered

as indications of myofascial loads. In the latter, the proximal tendons of LG+PL were kept at L_{REF}, while the distal tendons of LG+PL and SO were repositioned together in steps of 1 mm from L_{REF} −3 mm increasing up to 1 mm over SO optimum length, which occurred at L_{REF} +2 mm in all animals (data shown in Bernabei et al. 2015).

Data analysis

Analysis and results of SO fascicle length and SO tendon force will be described here. Results regarding LG muscle belly length as well as proximal and distal tendon forces of LG+PL do not directly address the aims of this study and are, therefore, presented in Supplementary Materials.

SO fascicle length

SO fascicle lengths (L_{SO}) were recorded assuming a speed of sound within vertebrate skeletal muscles of 1590 m/s (Marsh 2016) and were low-pass filtered (second-order Butterworth, 50 Hz cut-off). Recorded time-series were adjusted, because different values at L_{REF} were observed between set-ups. This was likely caused by slight changes in the orientation of the sonomicrometry crystals. To allow comparisons between set-ups, the inter-crystal distance measured in the passive muscle, excised after completion of the terminal experiment, was assumed to correspond to the shortest passive L_{SO} found among all four protocols (either ankle joint manipulation, knee joint manipulation, proximal LG+PL repositioning, or distal LG+PL+SO repositioning). Any length difference was added to all time-series of that specific protocol only. Then, the adjusted passive L_{SO} at L_{REF} within that specific protocol was used to adjust the time-series of the remaining protocols such that passive L_{SO} at L_{REF} in all four protocols were matched. Passive and active L_{SO} were calculated as the mean over a 50 ms time window during passive muscle conditions and during maximal excitation of all plantar–flexor muscles, respectively. Passive and active L_{SO} was calculated relative to its length at L_{REF}. No reliable L_{SO} could be obtained from rat CO-4.

Isometric SO tendon force

Passive and total isometric tendon forces were calculated over the same 50 ms time windows used to calculate passive and active L_{SO}. We assessed changes in force exerted at the distal tendon of SO (F_{SO}) with SO kept at a constant length as estimates of intermuscular mechanical interaction (Bernabei et al. 2015). Total F_{SO} values were normalized to the total force measured at L_{REF} (0.85 N, 0.26 N, 0.86 N, 1.05 N, and 0.91 N for TI-1, TI-2, TI-3, CO-4, and CO-5, respectively).

Statistics

Two-way repeated measures ANOVAs (SPSS Statistics 24, IBM Corporation, Armonk, NY, USA) were used to test for effects of the combination of muscle activation and MTU length changes obtained with either (1) knee angle changes, (2) ankle angle changes, (3) proximal LG+PL displacement, and (4) distal LG+PL+SO displacement on L_{SO}. One way repeated measures ANOVAs were used to test for effects of the same MTU length changes (1–4) on passive F_{SO} and on normalized total F_{SO}. Because of the small number of animals, no group comparison could be made between the tissue-integrated and control rats.

Results

Effects of joint angle on SO fascicle length

No main effect of knee angle (causing MTU length changes of the GA and PL complex, but not of SO) on SO fascicle length (L_{SO}) was found ($P = 0.964$, Fig. 2A). A main effect of activation on L_{SO} was found (mean across knee angles [normalized to the total force measured at reference length (L_{REF})]: 1.00 ± 0.01 L_{REF} and 0.95 ± 0.01 L_{REF} for passive and active muscle condition, respectively; $P = 0.005$), but without an interaction effect with knee angle ($P = 0.567$). For comparison, decreasing ankle angle (i.e., ankle dorsiflexion), corresponding to distal lengthening of all plantar–flexor muscles, resulted in significant main effects of ankle angle ($P < 0.001$) and muscle activation ($P = 0.007$) as well as a significant interaction effect ($P = 0.032$). Ankle dorsiflexion caused an average increase in L_{SO} from 0.89 ± 0.07 L_{REF} at 130° to 1.11 ± 0.2 L_{REF} at 70° ankle angle for passive muscle conditions and from 0.78 ± 0.04 L_{REF} at 130° to 1.07 ± 0.03 L_{REF} at 70° ankle angle for active muscle conditions (Fig. 2B). These results indicate that length changes of SO fascicles as a function of knee angle were <1% of the length changes of SO fascicles that occurred in response to changes in ankle angle (i.e., changes in MTU length of SO).

Effects of MTU length changes on SO fascicle length

Varying the proximal position of the tendons of the lateral GA and PL (LG+PL) did not affect L_{SO} ($P = 0.559$, Fig. 3A). In contrast, a main effect of activation on L_{SO} was found (mean across LG+PL MTU lengths: 1.00 ± 0.01 L_{REF} and 0.91 ± 0.01 L_{REF} for passive and active muscle condition, respectively;

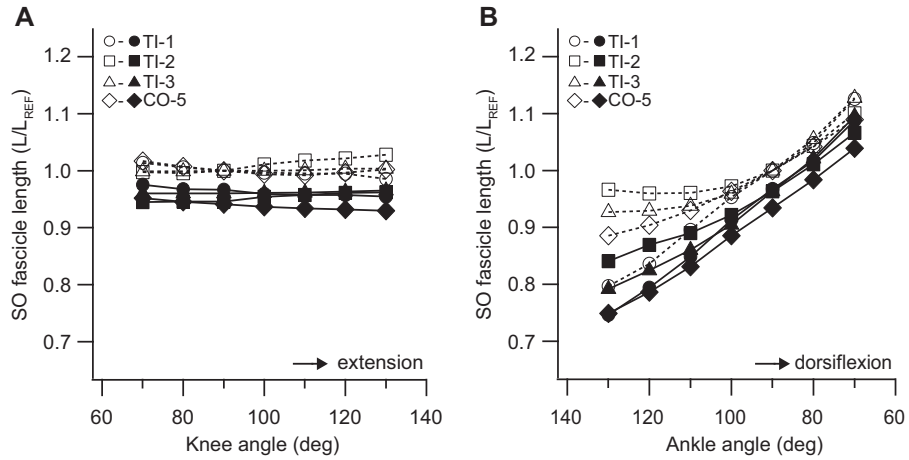

Fig. 2 Effects of joint angle on SO fascicle length. Normalized SO fascicle length (L/L_{REF}) for passive (open symbols) and active (closed symbols) muscle conditions during changes in knee angle (**A**) and ankle angle (**B**). No obvious differences were observed between the animals. Note that changes in knee angle affected the length of SO fascicles minimally, while a decrease in ankle angle (i.e., ankle dorsiflexion) increased the length of SO fascicles substantially. Data of individual rats are shown ($n = 4$).

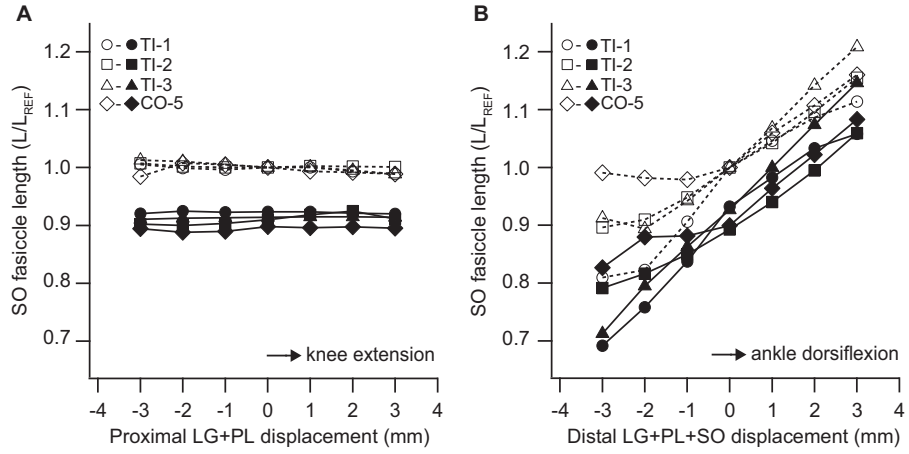

Fig. 3 Effects of MTU length changes on SO fascicle length. Normalized SO fascicle length (L/L_{REF}) for passive (open symbols) and active (closed symbols) muscle conditions with repositioning (**A**) the proximal tendons of the lateral GA and PL (LG+PL) complex and (**B**) the distal tendons of LG+PL+SO. No obvious differences were observed between the animals. Note that changes in proximal LG+PL position did not affect the MTU length of SO. Data of individual rats are shown ($n = 4$).

$P < 0.001$). Although a significant interaction effect was found ($P = 0.014$), *post hoc* analysis showed no effect of MTU length changes of LG+PL on L_{SO}, neither for passive (from 0.99 ± 0.01 L_{REF} at $+3$ mm to 1.00 ± 0.01 L_{REF} at -2 mm; $P = 0.083$) nor for active (from 0.90 ± 0.02 L_{REF} at -2 mm to 0.91 ± 0.01 L_{REF} at $+2$ mm; $P = 0.110$) muscle conditions. Similar to the effect of ankle angle on L_{SO}, substantially larger length changes were found with displacement of the distal tendons of LG+PL+SO rather than displacement of the proximal tendons of LG+PL (Fig. 3B). ANOVA showed significant main effects for position of distal LG+PL+SO tendons ($P < 0.001$) and muscle activation ($P = 0.001$) as well as a significant interaction effect ($P = 0.001$). L_{SO} changed from 0.90 ± 0.06 L_{REF} at -3 mm to 1.13 ± 0.07 L_{REF} at $+3$ mm for passive conditions, and from 0.78 ± 0.08 L_{REF} at -3 mm to 1.07 ± 0.05 L_{REF} at $+3$ mm for active conditions. Overall, these results show limited length changes of SO fascicles as a function of relative displacement of synergistic muscles.

Effects of MTU length changes on SO tendon force

Displacement of the proximal tendons of LG+PL significantly increased passive tendon force of SO (F_{SO}, $P < 0.001$) from 4.6 ± 1.7 mN at -3 mm to 8.4 ± 1.5 mN at $+3$ mm and increased normalized total F_{SO} from 0.7 ± 0.1 at -3 mm to 1.7 ± 0.6 at

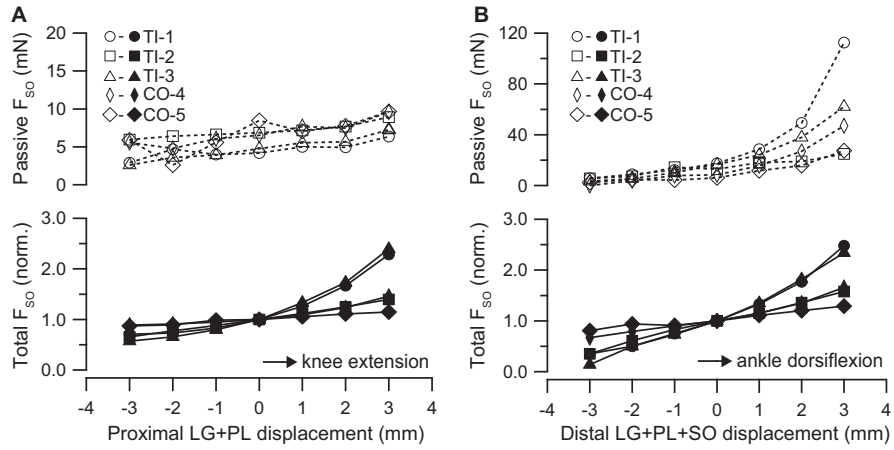

Fig. 4 Effects of MTU length changes on SO tendon force. SO tendon force (F_{SO}) for passive (upper panels, note the different *y*-axis ranges) and active (lower panels) muscle conditions as a function of the position of (**A**) the proximal tendons of the lateral GA and PL (LG+PL) complex and (**B**) the distal tendons of LG+PL+SO. Note that repositioning the proximal tendons of LG+PL did not affect the MTU length of SO. Data of individual rats are shown ($n = 5$).

+3 mm ($P < 0.001$, Fig. 4A). Mimicking ankle dorsiflexion (Fig. 4B), displacement of the distal tendons of LG+PL+SO increased passive F_{SO} from 3.4 ± 2.4 mN at −3 mm to 54.8 ± 35.7 mN at +3 mm ($P < 0.001$) and increased normalized total F_{SO} from 0.5 ± 0.3 at −3 mm to 1.9 ± 0.5 at +3 mm ($P < 0.001$). The increase in normalized total F_{SO} was higher for rat TI-1 and rat TI-3, which were both implanted with a tissue-integrating mesh. Although rat TI-2 was also implanted with a mesh, the effects of proximal LG+PL position on F_{SO} were very similar to the control animals (CO-4 and CO-5), showing a somewhat lower, but still significant ($n = 3$, $P < 0.001$) increase, i.e., from 0.8 ± 0.1 at −3 mm to 1.3 ± 0.2 at +3 mm. Changes in F_{SO} as a function of displacement of proximal LG+PL tendons were 9% (for passive) and 71% (for active muscle conditions) of the changes in F_{SO} that occurred during actual MTU length changes of SO. These results indicate substantial mechanical interaction between plantar–flexion muscles, especially during active muscle conditions.

Discussion

This is the first experimental study to simultaneously measure muscle forces and changes in fascicle length due to myofascial loads. We report evidence of mechanical interaction between SO and its synergists, but with only minimal length changes of SO fascicles, even when the extent of myofascial loads was enhanced by artificially increasing the stiffness of intermuscular connective tissues. These results suggest that effects of epimuscular myofascial loads on the mechanical function of muscles, when present, can occur without fascicle length changes.

Fascicle length changes caused by myofascial loads

Epimuscular myofascial loads are defined as forces exerted on the muscle belly surface (epimysium) of a muscle via connective tissues linked to neighboring muscles and non-muscular surrounding structures, such as blood vessels and nerves (Huijing 2009; Maas and Sandercock 2010). Previous invasive experiments performed on several muscle groups of animals have shown substantial changes of muscle forces exerted at the tendons due to myofascial loads elicited by repositioning a single muscle relative to adjacent ones (Huijing 2009). Although part of those results could be ascribed to the supra-physiological MTU length changes that were imposed, significant mechanical interaction was also found in studies that kept MTU length changes within physiological ranges (Bernabei et al. 2015). However, when replicating the paradigm used for animal studies in humans, conflicting results have been reported. By changing the length of two-joint muscles and measuring the longitudinal deformations on the adjacent one-joint muscle using ultrasound imaging, knee extension was found to decrease SO fascicle length (Tian et al. 2012), to decrease or increase (inconsistent between subjects) SO fascicle lengths (Diong and Herbert 2015), or have no effect on SO fascicle lengths (Kawakami et al. 1998; Tokuno et al. 2012). Because force measurements were not available in these human studies, the underlying assumption is that fascicle deformations, when present, were caused

by myofascial loads. However, this has never been tested.

In this study, we addressed the question whether myofascial loads exerted by neighboring muscles resulted in length changes of SO fascicles. Despite the low number of control animals, our results on tendon forces of SO during passive and active muscle conditions (Fig. 4A) confirm previous observations on a larger number of animals that received intermuscular connectivity enhancement (Bernabei et al. 2017a), thus supporting our conclusion that force transmission via myofascial pathways was increased in the group with enhanced connectivity measured here. The fact that we observed negligible length changes of SO fascicles across all animals makes our conclusion more robust with respect to pathological conditions when myofascial loads may have a larger impact on muscle function, for example in presence of scar tissues between muscles after surgery or injury (Bernabei et al. 2016, 2017a). Scar tissue after injury has been found to reduce local two-dimensional deformation of muscle tissue (Silder et al. 2010), resulting in high tissue strain in other regions that may increase the risk for re-injury. The present study did not measure deformations outside the longitudinal direction and local strains were not captured.

In contrast with our results, myofascial loads have been detected by muscle spindles within rat SO (Smilde et al. 2016), suggesting changes in fiber length. Although we measured the length of the whole SO muscle belly, the small pennation angle and simple architecture of SO in rats (Close 1964; Eng et al. 2008) indicate that the absence of muscle belly length changes also indicates an absence of fiber length changes. Importantly, the displacement of the distal tendon of the lateral GA and PL (LG+PL) relative to SO imposed in that study does not reflect the intact situation in which the distal tendons span the ankle joint and are repositioned together. Compared to our study, this could have resulted in higher loads via myofascial pathways, thus higher length changes, also because connective tissues between SO and LG+PL appear to be stiffer distally (see Fig. 8 in Bernabei et al. 2016). However, we cannot exclude the possibility of length changes of sarcomeres locally without changes in total fiber length (Maas and Huijing 2009; Tijs et al. 2015a), especially because proximal MTU length changes of LG+PL may result in loads exerted predominantly on the proximal part of the intermuscular pathway.

The present study shows substantial changes in muscle force without changes in fascicle length, which is a discrepancy if we consider a simple muscle model, composed of a contractile and a series elastic component only. For passive conditions, any change in force would imply a deformation of the elastic component. Additionally, the active force produced by the contractile element would be scaled from the force produced by a sarcomere, given its length. In such model, any myofascial loads will necessarily imply deformation of fascicles and length changes of sarcomeres locally, thus resulting in a change in net muscle force produced by the contractile element. Our results show that substantial myofascial loads exerted on SO were not accompanied by length changes of SO fascicles, therefore offering some evidence for ruling out this paradigm. An alternative view should consider the complex architecture of connective tissue linkages between muscles. In this view, connective tissues linking epimysia of neighboring muscles, running parallel to the series of sarcomeres and linking tendons of adjacent muscles directly, could serve as an additional pathway for force transmission. Such pathway could be deformed by shear between muscles, given by relative displacement or bulging, thus implying a displacement of adjacent aponeuroses of neighboring muscles, without any length changes in sarcomeres locally. As a result, force produced by the contractile elements would be unaffected. Using finite element models of linked models that account for elastic deformation of the extracellular matrix, large effects of myofascial loads on the distribution of sarcomere length were predicted when the muscle of interest was kept at high muscle length, but only small effects were predicted for low muscle lengths (Yucesoy et al. 2006). Thus, providing some evidence that supports this alternative explanation for the effects of epimuscular myofascial loads.

Implications for human studies

Our present results cannot provide a definitive answer to the question whether myofascial loads caused the muscle deformations found *in vivo* in humans. However, they may help explaining seemingly opposite results found when investigating myofascial loads with non-invasive imaging techniques. We have shown that myofascial loads can occur without changes in fascicle length. However, we did not have information regarding shear and displacement between aponeuroses of adjacent muscles or muscle deformations locally. In addition, local measures of muscle stiffness *in vivo* in humans assessed using non-invasive techniques such as ultrasound shear wave elastography (Bouillard et al. 2011; Gennisson et al. 2013) could be used to provide more

information on the relationship between local deformations and myofascial loads.

It can be readily understood that the presence of a common tendon between two adjacent muscles may compensate or mask effects of myofascial loads (Tijs et al. 2014; Bojsen-Møller and Magnusson 2015; Finni et al. 2018). For example, when imaged with ultrasound, SO fascicles have been reported to elongate, rather than shorten, with shortening GA during passive knee flexion (Tian et al. 2012). A possible explanation is that the length of SO fascicles could change in response to changes in LG length, not caused by myofascial loads, but by mechanical interaction via the common Achilles tendon. When myofascial loads have been assessed in the intact triceps surae of rats (Tijs et al. 2015b) and cats (Maas and Sandercock 2008) by measuring joint torques, limited or no effects at the joint have been observed, potentially because myofascial effects could be masked by mechanical interaction via the common Achilles tendon. In the current study, we found that length changes of synergistic muscles did not affect the length of SO fascicles, neither in a nearly intact hindlimb with an intact Achilles tendon nor in a disrupted compartment with its subtendons isolated, thus disproving the possibility of the common tendon compensating the effects of myofascial loads. As such a comparison is not possible in human experiments, it is hard to assess whether mechanical interactions via a common tendon mask those related to myofascial loads between muscle bellies.

Conclusions

Our study showed no length changes in SO fascicles despite significant mechanical interaction between SO and its synergistic muscles. Therefore, we conclude that myofascial loads can occur without fascicle length changes, suggesting that the observed changes in forces exerted at the tendons were the result of forces transmitted from surrounding muscles rather than due to changes in the force generating capacity of a muscle.

Acknowledgments

We thank Frans den Boer for the implantable connectors used for sonomicrometry. We further thank Guus Baan and Wendy Noort for their assistance with survival surgeries.

Funding

This work was supported by the Division for Earth and Life Sciences of the Netherlands Organization for Scientific Research [864-10-011 to H.M.]. M.B. is currently supported by the National Institutes of Health [grant 5R01-AR-071162-02] to Eric J. Perreault. C.T. is currently supported by the National Institutes of Health [grant AR055648] to Andrew A. Biewener.

Supplementary data

Supplementary data available at *ICB* online.

References

Berkenhout J. 1769. Outlines of the natural history of Great Britain and Ireland. In three volumes. Vol. I. Comprehending the animal kingdom. - pp. XIII + 233 pp. London. (Elmsly). (http://resolver.sub.uni-goettingen.de/purl?PPN367209748). Digitized 2003-10-08.

Bernabei M, Maas H, van Dieën JH. 2016. A lumped stiffness model of intermuscular and extramuscular myofascial pathways of force transmission. Biomech Model Mechanobiol 15:1747–63.

Bernabei M, van Dieën JH, Baan GC, Maas H. 2015. Significant mechanical interactions at physiological lengths and relative positions of rat plantar flexors. J Appl Physiol 118:427–36.

Bernabei M, van Dieën JH, Maas H. 2017a. Altered mechanical interaction between rat plantar flexors due to changes in intermuscular connectivity. Scand J Med Sci Sports 27:177–87.

Bernabei M, van Dieën JH, Maas H. 2017b. Evidence of adaptations of locomotor neural drive in response to enhanced intermuscular connectivity between the triceps surae muscles of the rat. J Neurophysiol 118:1677–89.

Bernabei M, van Dieën JH, Maas H. 2017c. Longitudinal and transversal displacements between triceps surae muscles during locomotion of the rat. J Exp Biol 220:537–50.

Bojsen-Møller J, Magnusson SP. 2015. Heterogeneous loading of the human Achilles tendon in vivo. Exerc Sport Sci Rev 43:190–7.

Bojsen-Møller J, Schwartz S, Kalliokoski KK, Finni T, Magnusson SP. 2010. Intermuscular force transmission between human plantarflexor muscles in vivo. J Appl Physiol 109:1608–18.

Bouillard K, Nordez A, Hug F. 2011. Estimation of individual muscle force using elastography. PLoS One 6:e29261.

Close R. 1964. Dynamic properties of fast and slow skeletal muscles of the rat during development. J Physiol 173:74–95.

Diong J, Herbert RD. 2015. Is ankle contracture after stroke due to abnormal intermuscular force transmission? J Appl Biomech 31:13–8.

Eng CM, Smallwood LH, Rainiero MP, Lahey M, Ward SR, Lieber RL. 2008. Scaling of muscle architecture and fiber types in the rat hindlimb. J Exp Biol 211:2336–45.

Finni T, Bernabei M, Baan GC, Noort W, Tijs C, Maas H. 2018. Non-uniform displacement and strain between the soleus and gastrocnemius subtendons of rat Achilles tendon. Scand J Med Sci Sports 28:1009–17.

Finni T, Cronin NJ, Mayfield D, Lichtwark GA, Cresswell AG. 2017. Effects of muscle activation on shear between human soleus and gastrocnemius muscles. Scand J Med Sci Sports 27:26–34.

Gennisson J-L, Deffieux T, Fink M, Tanter M. 2013. Ultrasound elastography: principles and techniques. Diagn Interv Imaging 94:487–95.

Greene EC. 1935. Anatomy of the rat. Trans Am Phil Soc 27:1–370.

Huijing PA. 1995. Parameter interdependence and success of skeletal muscle modelling. Hum Mov Sci 14:443–86.

Huijing PA. 2009. Epimuscular myofascial force transmission: a historical review and implications for new research. International Society of Biomechanics Muybridge Award Lecture, Taipei, 2007. J Biomech 42:9–21.

Huijing PA, Baan GC. 2001. Extramuscular myofascial force transmission within the rat anterior tibial compartment: proximo-distal differences in muscle force. Acta Physiol Scand 173:297–311.

Johnson WL, Jindrich DL, Roy RR, Reggie Edgerton V. 2008. A three-dimensional model of the rat hindlimb: musculoskeletal geometry and muscle moment arms. J Biomech 41:610–9.

Kawakami Y, Ichinose Y, Fukunaga T. 1998. Architectural and functional features of human triceps surae muscles during contraction. J Appl Physiol 85:398–404.

Maas H, Baan GC, Huijing PA. 2001. Intermuscular interaction via myofascial force transmission: effects of tibialis anterior and extensor hallucis longus length on force transmission from rat extensor digitorum longus muscle. J Biomech 34:927–40.

Maas H, Baan GC, Huijing PA. 2004. Muscle force is determined also by muscle relative position: isolated effects. J Biomech 37:99–110.

Maas H, Gregor RJ, Hodson-Tole EF, Farrell BJ, Prilutsky BI. 2009. Distinct muscle fascicle length changes in feline medial gastrocnemius and soleus muscles during slope walking. J Appl Physiol 106:1169–80.

Maas H, Huijing PA. 2009. Synergistic and antagonistic interactions in the rat forelimb: acute effects of coactivation. J Appl Physiol 107:1453–62.

Maas H, Huijing PA. 2011. Myofascial force transmission between transferred rat flexor carpi ulnaris muscle and former synergistic palmaris longus muscle. Muscles Ligaments Tendons J 1:127–33.

Maas H, Huijing PA. 2012a. Mechanical effect of rat flexor carpi ulnaris muscle after tendon transfer: does it generate a wrist extension moment?. J Appl Physiol 112:607–14.

Maas H, Huijing PA. 2012b. Effects of tendon and muscle belly dissection on muscular force transmission following tendon transfer in the rat. J Biomech 45:289–96.

Maas H, Sandercock TG. 2008. Are skeletal muscles independent actuators? Force transmission from soleus muscle in the cat. J Appl Physiol 104:1557–67.

Maas H, Sandercock TG. 2010. Force transmission between synergistic skeletal muscles through connective tissue linkages. J Biomed Biotechnol 2010:575672.

Marsh RL. 2016. Speed of sound in muscle for use in sonomicrometry. J Biomech 49:4138–41.

Silder A, Reeder SB, Thelen DG. 2010. The influence of prior hamstring injury on lengthening muscle tissue mechanics. J Biomech 43:2254–60.

Smilde HA, Vincent JA, Baan GC, Nardelli P, Lodder JC, Mansvelder HD, Cope TC, Maas H. 2016. Changes in muscle spindle firing in response to length changes of neighboring muscles. J Neurophysiol 115:3146–55.

Tian M, Herbert RD, Hoang P, Gandevia SC, Bilston LE. 2012. Myofascial force transmission between the human soleus and gastrocnemius muscles during passive knee motion. J Appl Physiol 113:517–23.

Tijs C, van Dieën JH, Baan GC, Maas H. 2014. Three-dimensional ankle moments and nonlinear summation of rat triceps surae muscles. PLoS One 9:e111595.

Tijs C, van Dieën JH, Maas H. 2015a. Effects of epimuscular myofascial force transmission on sarcomere length of passive muscles in the rat hindlimb. Physiol Rep 3:e12608.

Tijs C, van Dieën JH, Maas H. 2015b. No functionally relevant mechanical effects of epimuscular myofascial connections between rat ankle plantar flexors. J Exp Biol 218:2935–41.

Tokuno CD, Lichtwark GA, Cresswell AG. 2012. Modulation of the soleus H-reflex during knee rotations is not consistent with muscle fascicle length changes. Eur J Appl Physiol 112:3259–66.

Yucesoy CA, Huijing PA. 2012. Specifically tailored use of the finite element method to study muscular mechanics within the context of fascial integrity: the linked fiber-matrix mesh model. Int J Multiscale Comput Eng 10:155–70.

Yucesoy CA, Maas H, Koopman BHF, Grootenboer HJ, Huijing PA. 2006. Mechanisms causing effects of muscle position on proximo-distal muscle force differences in extra-muscular myofascial force transmission. Med Eng Phys 28:214–26.